Available online at www.sciencedirect.com
ScienceDirect
Journal of Sound and Vibration 322 (2009) 490–512
JOURNAL OF SOUND AND VIBRATION
www.elsevier.com/locate/jsvi

Discrete breathers and nonlinear normal modes in monoatomic chains

G.M. Chechin*, G.S. Dzhelauhova

Southern Federal University (Former Rostov State University), Zorge Street, 5, Rostov-on-Don, Russia

Accepted 2 April 2008
The peer review of this article was organised by the Guest Editor
Available online 2 June 2008

Abstract

We consider a relation between discrete breathers (DBs) and nonlinear normal modes in some nonlinear monoatomic chains. The dependence of the breathers' stability on the strength of interparticle interaction in the K_4 chain (the chain with uniform on-site and intersite potentials of the fourth order) is investigated. A general method for constructing DBs which provides the pair synchronization between the individual particles' vibrations is discussed. Many-frequency breathers as DBs of a new type and quasibreathers [introduced in *Physical Review E* 74 (2006) 036608] are analyzed.

1. Introduction

Over two last decades, discrete breathers (DBs) (intrinsic localized modes) have attached enormous attention in many areas of physics. They represent spatially localized and time periodic excitations in nonlinear Hamiltonian lattices. Different aspects of these dynamical objects were analyzed in various physical systems by mathematical, numerical and experimental methods (see review papers [1–5] and references therein). Note that DBs were studied in microscopic systems (antiferromagnetic spin–lattices [6], Bose–Einstein condensates [7,8] etc.), in mesoscopic systems (arrays of Josephson junctions [9,10], micromechanical cantilever arrays [11,12], etc.) and even in some macroscopic lattices, such as electrical transmission lines [13]. A possible role of DBs in some biological processes, especially, in the DNA molecule and motor proteins are also widely discussed in the literature [14–17]. A great number of papers were devoted to study of the moving breathers (see Refs. [18–23] and many other works cited in Refs. [1–4]). Recently, some new types of DBs have been investigated by different authors in 1D, 2D and 3D structures [5]. For example, let us refer to the wandering breathers in weakly coupled nonlinear chains [24].

Rigorous existence proofs of DBs as strictly time periodic objects in networks of weakly coupled anharmonic oscillators can be found in Refs. [1–4]. In Ref. [25], some physical arguments for the possibility of energy localization in uniform nonlinear lattices were presented by Ovchinnikov many years before the conventional definition of the DBs was introduced.

*Corresponding author.
E-mail address: chechin@aaanet.ru (G.M. Chechin).

0022-460X/$ - see front matter © 2008 Elsevier Ltd. All rights reserved.
doi:10.1016/j.jsv.2008.04.002

Several numerical schemes for obtaining DBs with high precision were developed in Refs. [26,27] (see also Refs. [3,4]).

Actually, the possibility of existence of DBs as *strictly* time-periodic entities is not trivial because, as a consequence of their spatial localization, individual particles vibrate with essentially different amplitudes but with the same frequency.

In Ref. [28], we have analyzed some localized dynamical objects which are considered in the literature as DBs and found that they are not strictly time-periodic entities: there are *slight deviations* in the frequencies of the individual particles. Such objects we call *quasibreathers*.[1] Moreover, it is possible to ascribe some numerical characteristics (for example, the mean square deviation of the frequencies of individual particles) to a given quasibreather which determine a degree of its nearness to an exact breather.

In contrast to the exact breathers, quasibreathers seem to be more adequate dynamical objects because the former are practically impossible to create in any physical experiments.

In some rare cases, exact DBs can be constructed numerically in terms of nonlinear normal modes (NMs) as introduced by Rosenberg in Ref. [30]. In Ref. [28] we have proceeded in such a way for the K_4 chain (monoatomic chain with uniform on-site and intersite potentials of the fourth order). Some analytical results on the existence and stability of the DBs can be obtained for this chain. In Ref. [28], we have analyzed the stability of the symmetric breather (Sievers–Takeno mode) as a function of the relative strength (β) of the intersite potential with respect to the on-site potential. In the present paper, we extend this analysis to the breathers of some other types in the K_4 chain and in the chain of the Duffing oscillators with cubic coupling. In both cases, the concept of nonlinear normal modes is used for DBs' constructing in Section 2.

On the other hand, it is well known that nonlinear normal modes cannot exist for a majority of the N-particle mechanical systems. Indeed, the vibrational regime associated with a nonlinear normal mode must satisfy a very hard condition: the displacement of every particle at any instant t is proportional to the displacement of a given, arbitrarily chosen particle. From this condition, it follows that all the particles of the mechanical system vibrate with identical frequencies.

However, the above condition is *not necessary* for DBs' existence. For this purpose, it is sufficient that the evolution of displacements of all the particles are described by time-periodic functions with the same frequency (without their proportionality at any instant).

Such more soft conditions can be satisfied by the pair synchronization method developed in Refs. [31,32]. It represents an iterative procedure for synchronization of each pairs of adjacent particles. The pair synchronization method (PS method) can be applied to construct breather solutions to dynamical equations for arbitrary nonlinear Hamiltonian lattices, but we prefer to illustrate it with the chain of the linear coupled Duffing oscillators (Section 3).

With the aid of this method, we can construct DBs even for sufficiently strong interparticle interactions. The stability of the obtained breathers can be analyzed by the Floquet method.

In Section 4, we consider DBs of a new type which we call ''many-frequency'' breathers. Being strictly time-periodic, they differ from the conventional DBs by the following property: the particles in the many-frequency breather vibrate with *different* but *commensurate* frequencies. A possibility of the existence of such dynamical objects has been slightly mentioned in [1] in connection with the construction of *multibreathers*, but we are not aware of any detailed discussion about many-frequency DBs. Moreover, we think that many-frequency breathers could not be considered as a special case of the multibreathers. Indeed, the main property of the latter is that several particles in the breather vibration possess significant amplitudes. These amplitudes can be obtained in the so-called anticontinuous limit by fixing the appropriate coding sequence which implies that several particles have been excited when the interparticle interaction is absent (for more detail see papers [1,3]).

We discuss the many-frequency breathers for the linear coupled Duffing oscillators, where nonlinear normal modes do not exist, as well as for the K_4 chain and for the chain of Duffing oscillators with cubic coupling in which nonlinear normal modes do exist. The matter of fact is that, in spite of existence of nonlinear normal modes in the latter systems, the many-frequency breathers *do not* represent modes of this type.

[1]We distinguish between quasibreathers and *quasiperiodic breathers* (see, for example, Ref. [29]) for which several incommensurate frequencies with significant amplitudes are presented in the Fourier spectrum.

In Conclusion, we sum the above results and consider some perspectives for studying stationary DBs and quasibreathers which appear when we do not achieve the strict synchronization in vibrations of all the individual particles.

It has been already mentioned that the concepts of quasibreathers and many-frequency breathers, as well as the pair synchronization method are valid (at least, in principle!) for arbitrary nonlinear Hamiltonian lattices. Nevertheless, we will demonstrate them using the following simple mechanical models.

1. The chain of linear coupled hard Duffing oscillators (LD model):

$$\ddot{x}_i + x_i + x_i^3 = \beta[x_{i+1} - 2x_i + x_{i-1}]. \tag{1}$$

2. The chain of the hard Duffing oscillators with cubic coupling (CD model):

$$\ddot{x}_i + x_i + x_i^3 = \beta[(x_{i+1} - x_i)^3 - (x_i - x_{i-1})^3]. \tag{2}$$

3. The K_4 chain:

$$\ddot{x}_i + x_i^3 = \beta[(x_{i+1} - x_i)^3 - (x_i - x_{i-1})^3]. \tag{3}$$

The periodic boundary conditions

$$x_{N+1}(t) = x_1(t), \quad x_0(t) = x_N(t) \tag{4}$$

are supposed to be fulfilled for all the above listed dynamical equations (1)–(3).

Note that models (1)–(3) can be applied to studying breathers in certain mechanical systems, in particular, Eq. (1) were used in Ref. [12] for modeling breather-like dynamical objects in cantilever arrays. We consider Eqs. (1)–(3) as abstract dynamical models, but discussing the methods for their solving and the appropriate numerical results, we will treat $x_i(t)$ as displacements of the individual particles (from their equilibrium positions) in a certain ''monoatomic chain''.

2. Localized nonlinear normal modes as DBs

2.1. DBs in the K_4 chain

First of all, let us note that models similar to the K_4 chain (3) have been considered in the papers [26,27,33–36], but we analyze this chain with a different purpose and in a different manner. A comparison of our results with those obtained in the above papers can be found in Ref. [28].

Below we reproduce some results and methods from our paper [28] which are necessary for the further discussion.

According to the definition of the similar nonlinear normal modes introduced by Rosenberg in Ref. [30], displacements $x_i(t)$ of all the particles of a given mechanical system are proportional to the displacement $x_1(t)$ of the first particle for any instant t:

$$x_i(t) = k_i x_1(t), \quad i = 1..N \ \ (k_1 = 1). \tag{5}$$

Substituting expressions (5) into equation of motion (3) for the K_4 chain, we obtain N differential equations with respect to the same function $x_1(t)$. Demanding all these equations to be identical, we find $(N-1)$ nonlinear algebraic equations for $(N-1)$ coefficients $k_2, k_3, \ldots, k_N$ from Eq. (5) and one differential equation for $x_1(t)$ which is called governing equation. The set $\mathbf{k} = \{k_1, k_2, k_3, \ldots, k_N\}$ determines the *shape* of nonlinear normal mode or its *spatial profile*.

The above-mentioned algebraic equations for the K_4 chain, can be written as follows:

$$k_i^3 + \beta[(k_{i+1} - k_i)^3 - (k_i - k_{i-1})^3] = k_i\{1 + \beta[(k_2 - 1)^3 - (1 - k_N)^3]\} \quad (i = 2..N), \tag{6}$$

Table 1
Spatial profiles $\{\ldots,\xi_3,\xi_2,\xi_1,\xi_0,\xi_1,\xi_2,\xi_3,\ldots\}$ of symmetric breathers in the K_4-chain with $N=5,9,15$ particles for $\beta=0.3$

	$N=5$	$N=9$	$N=15$
ξ_0	1	1	1
ξ_1	−0.2992883116	−0.2992883120	−0.2992883120
ξ_2	0.0035993414	0.0035993477	0.0035993477
ξ_3		$-0.6040174714\times10^{-8}$	$-0.6040174714\times10^{-8}$
ξ_4		*	*
ξ_5			*
ξ_6			*
ξ_7			*

while the governing equations is

$$\ddot{x}_1 + p^2(\mathbf{k})\cdot x_1^3 = 0. \tag{7}$$

There are some localized and delocalized nonlinear normal modes among the solution of Eqs. (6). Obviously, the former represent DBs.

Below we discuss some specific types of DBs in the K_4 chain determined by the following spatial profiles $\mathbf{k}=\{k_1,k_2,k_3,\ldots,k_N\}$:

(i) symmetric breather (Sievers–Takeno mode)

$$\mathbf{k}=\{\ldots,\xi_3,\xi_2,\xi_1,1,\xi_1,\xi_2,\xi_3,\ldots\}; \tag{8}$$

(ii) antisymmetric breather (Page mode)

$$\mathbf{k}=\{\ldots,-\xi_3,-\xi_2,-\xi_1,-1,1,\xi_1,\xi_2,\xi_3,\ldots\}; \tag{9}$$

(iii) symmetric multibreather

$$\mathbf{k}=\{\ldots,\xi_3,\xi_2,\xi_1,1,1,\xi_1,\xi_2,\xi_3,\ldots\}. \tag{10}$$

Here ξ_i must be found as solutions to algebraic equations (6). [Note that by substituting these profiles into system (6) we reduce its dimension.]

We use the mathematical package MAPLE for solving Eqs. (6) with specification Digits = 20 and, therefore, the spatial profile of the DBs which are presented below turn out to be *practically exact*.

Note that Eqs. (6) possess many different solutions. Taking into account that we search for DBs which represent spatially localized dynamical objects, some restrictions have been imposed on the variables ξ_i $(i=1,2,3,\ldots)$ from Eqs. (8)–(10): $|\xi_{i+1}|<|\xi_i|<1$. These relations reduce considerably the number of admissible solutions of Eqs. (6).

Due to the periodic boundary conditions (4), we can imagine that our monoatomic chain represents a *ring* with N particles. Subsequently increasing N, we find the DB of a given type for more and more long chains.

2.1.1. Symmetric breathers (Sievers–Takeno modes)

Some results of our calculations for the symmetric breather (8) are presented in Table 1. Comparing the profiles for the chain with $N=3,5,7,9,11$, etc. particles, one can reveal that the results for $N=15$ are practically exact and the further increase of N does not affect the spatial profile of the breather solution. Indeed, the considered breather demonstrates such a strong localization that the displacement of the particles which are more than three lattice spacings distance from the breather center are utterly insignificant (they do not exceed 10^{-20} and we denote them in our tables by an asterisk). Therefore, we

conclude that the profile for $N = 19$ (and even for $N = 5$) can be considered as the profile for the infinite chain ($N = \infty$).[2]

The time dependence of the breather solution is determined by the governing equation (7). For the symmetric breather (8), in Ref. [28], we have found the following values of $p^2(N)$ for different N ($\beta = 0.3$):

$$p^2(3) = 2.2983734518,$$

$$p^2(5) = 2.3160362290,$$

$$p^2(7) = 2.3160362301,$$

$$p^2(9) = 2.3160362301.$$

For initial conditions

$$x_1(0) = A_0, \quad \dot{x}_1(0) = 0 \tag{11}$$

the solution to Eq. (7) (see, for example, Ref. [33]) reads

$$x_1(t) = A_0 cn(\omega t, \tfrac{1}{\sqrt{2}}), \tag{12}$$

where the frequency ω is the linear function of the amplitude A_0:

$$\omega = pA_0. \tag{13}$$

Here $cn(\omega t, m)$ is the Jacobi elliptic function with the modulus m equal to $\frac{1}{\sqrt{2}}$. Note that such a value of the modulus is needed to eliminate the linear term, because, in the general case, the function $cn(\tau, m)$ satisfies the equation[3]:

$$cn''(\tau, m) + [1 - 2m^2]cn(\tau, m) + 2m^2 cn^3(\tau, m) = 0.$$

Introducing the new time and space variables τ, $x(\tau)$ according to relations

$$t = \frac{\tau}{pA_0}, \quad x_1(t) = A_0 x(\tau), \tag{14}$$

we obtain from Eqs. (7) and (11) the following Cauchy problem for the function $x(\tau)$[4]:

$$x'' + x^3(\tau) = 0, \quad x(0) = 1, \;\; x'(0) = 0 \tag{15}$$

with the solution

$$x(\tau) = cn(\tau, \tfrac{1}{\sqrt{2}}). \tag{16}$$

In conclusion, it is worth emphasizing that the spatial profile provided in Table 1 turns out to be *universal* for the breathers with different amplitudes A_0 (it does not depend on the amplitude), while the breather frequency depends on A_0 linearly ($\omega = pA_0$).

Now let us discuss the stability of the symmetric breather in the K_4 chain following the paper [28].

In accordance with the standard prescription of the linear stability analysis, we linearize the nonlinear equations of motion (3) in the vicinity of the periodic regime described by our breather and investigate the resulting linear differential equations with time-periodic coefficients.

Let

$$\mathbf{x}_b(t) = \{k_1 x_1(t), k_2 x_1(t), \ldots, k_N x_1(t)\} \tag{17}$$

be the exact breather solution determined by Eqs. (5)–(7) and

$$\boldsymbol{\delta}(t) = \{\delta_1(t), \delta_2(t), \ldots, \delta_N(t)\} \tag{18}$$

[2]The breather space localization is usually characterized by an exponential decay of the vibrational amplitudes of the peripheral particles, but in the K_4 chain we have the superexponential decay in terms of the paper [36].

[3]This equation can be obtained using the elementary formulas for the Jacobi elliptic functions (see, for example, Ref. [37]).

[4]We denote the differentiation with respect to t by dot, while that with respect to τ by prime.

be an infinitesimal vector describing a deviation from $\mathbf{x}_b(t)$. Then we substitute the vector $\mathbf{x}(t) = \mathbf{x}_b(t) + \boldsymbol{\delta}(t)$ into Eqs. (3) and linearize these equations with respect to δ_j $(j = 1..N)$.

As a result of this procedure, we obtain the linearized system

$$\ddot{\boldsymbol{\delta}}(t) = -3x_1^2(t)\mathbf{A}\boldsymbol{\delta}(t), \tag{19}$$

where $\mathbf{A}$ is a symmetric matrix with time-independent coefficients.

The specific structure of the linearized system (19) allows us to make an essential step for simplifying the further stability analysis. Indeed, let us pass from the vector variable $\boldsymbol{\delta}(t)$ to a new variable $\tilde{\boldsymbol{\delta}}(t)$ whose definition involves a *time-independent* orthogonal matrix $\mathbf{S}$:

$$\boldsymbol{\delta}(t) = \mathbf{S}\tilde{\boldsymbol{\delta}}(t). \tag{20}$$

Substituting $\boldsymbol{\delta}$ in such form into Eq. (19) and multiplying this equation by the matrix $\tilde{\mathbf{S}}$ from the left ($\tilde{\mathbf{S}} = \mathbf{S}^{-1}$ is the transpose of $\mathbf{S}$), we obtain[5]

$$\ddot{\tilde{\boldsymbol{\delta}}} = -3x_1^2(t)(\tilde{\mathbf{S}}\mathbf{A}\mathbf{S})\tilde{\boldsymbol{\delta}}. \tag{21}$$

On the other hand, the matrix $\mathbf{A}$ is symmetric[6] and, therefore, there exists an orthogonal matrix $\mathbf{S}$ transforming the matrix $\mathbf{A}$ to a fully diagonal form $\mathbf{A}_{\text{diag}}$:

$$\tilde{\mathbf{S}}\mathbf{A}\mathbf{S} = \mathbf{A}_{\text{diag}}. \tag{22}$$

If we find such matrix $\mathbf{S}$, the linearized system (21) decomposes into N *independent* differential equations

$$\ddot{\tilde{\delta}}_j + 3x_1^2(t)\lambda_j\tilde{\delta}_j = 0, \quad j = 1..N, \tag{23}$$

where λ_j are the eigenvalues of the matrix $\mathbf{A}$. Moreover, solving the eigenproblem $\mathbf{A}\mathbf{y} = \lambda\mathbf{y}$ for the matrix $\mathbf{A}$, we obtain not only λ_j for Eq. (23), but also the explicit form of the matrix $\mathbf{S}$ from Eq. (20): its columns turn out to be the eigenvectors $\mathbf{y}_j$ $(j = 1..N)$ of the matrix $\mathbf{A}$.

In Eq. (23), each equation represents the linear differential equation with *time-periodic* coefficient. The most well-known differential equation of this type is the Mathieu equation

$$\ddot{z} + [a - 2q\cos(2t)]z = 0. \tag{24}$$

The $(a - q)$ plane for this equation splits into regions of stable and unstable motion [37]. If parameters (a,q) fall into a stable region, $z(t)$ that is small at the initial instant $t = 0$ continues to be small for all times $t > 0$ (the case of Lyapunov stability). Oppositely, if $z(0)$ is a small value (even infinitesimal), $z(t)$ will begin to grow rapidly for $t > 0$ (Lyapunov instability). Actually, we must analyze the stability of the *zero* solution of Eq. (24).

We can obtain some estimations for the stability regions of Eqs. (23) by reducing these equations to the Mathieu from in a certain approximation [28], but it is possible to investigate the stability of our breather rigorously. Indeed, substituting the exact breather solution from Eq. (12) into Eqs. (23), we transform them to the Lamé equation in the Jacobi form [38]:

$$z_j'' + \Lambda_j cn^2(\tau, \tfrac{1}{\sqrt{2}})z_j(\tau) = 0. \tag{25}$$

Here

$$z_j(\tau) = \tilde{\delta}_j\left(\frac{\tau}{pA_0}\right), \quad \Lambda_j = \frac{3\lambda_j}{p^2}, \quad \tau = pA_0 t \tag{26}$$

(A_0 is the amplitude of the central breather's particle).

[5]The tildes in $\tilde{\delta}$ and $\tilde{\mathbf{S}}$ are used in different sense: $\tilde{\boldsymbol{\delta}}$ is the new vector variable with respect to the old variable $\boldsymbol{\delta}$, while $\tilde{\mathbf{S}}$ is the transpose of $\mathbf{S}$.

[6]This property is a consequence of the fact that the linearized system (19) can be written in the form $\ddot{\boldsymbol{\delta}} = J(t)\boldsymbol{\delta}$ via the Jacobi matrix $J(t)$ which is constructed from the second partial derivatives of the total potential energy of the considered chain.

Table 2
Eigenvalues of the matrix **A** of the linearized dynamical system for the K_4 chain with different number of particles N ($\beta = 0.3$)

$N = 3$		$N = 5$	
$\lambda_1 = 2.298373452$	$\Lambda_1 = 3$	$\lambda_1 = 2.316036234$	$\Lambda_1 = 3$
$\lambda_2 = 0.5880160166$	$\Lambda_2 = 0.7675201995$	$\lambda_2 = 0.6248090298$	$\Lambda_2 = 0.8093254611$
$\lambda_3 = 0.2934494449$	$\Lambda_3 = 0.3830310231$	$\lambda_3 = 0.3226215801$	$\Lambda_3 = 0.4178970630$
		$\lambda_4 = 0.02626701223$	$\Lambda_4 = 0.03402409500$
		$\lambda_5 = 0.02530830363$	$\Lambda_5 = 0.03278226390$
$N = 7$		$N = 9$	
$\lambda_1 = 2.316036234$	$\Lambda_1 = 3$	$\lambda_1 = 2.316036234$	$\Lambda_1 = 3$
$\lambda_2 = 0.6248090398$	$\Lambda_2 = 0.8093254740$	$\lambda_2 = 0.6248090398$	$\Lambda_2 = 0.8093254740$
$\lambda_3 = 0.3226216094$	$\Lambda_3 = 0.4178971017$	$\lambda_3 = 0.3226216094$	$\Lambda_3 = 0.4178971017$
$\lambda_4 = 0.02627089232$	$\Lambda_4 = 0.03402912093$	$\lambda_4 = 0.02627089232$	$\Lambda_4 = 0.03402912093$
$\lambda_5 = 0.02531216336$	$\Lambda_5 = 0.03278726346$	$\lambda_5 = 0.02531216336$	$\Lambda_5 = 0.03278726346$
$\lambda_6 = 0.3886030305 \times 10^{-5}$	$\Lambda_6 = 0.5033639268 \times 10^{-5}$	$\lambda_6 = 0.3886030305 \times 10^{-5}$	$\Lambda_6 = 0.5033639268 \times 10^{-5}$
$\lambda_7 = 0.3886011392 \times 10^{-5}$	$\Lambda_7 = 0.5033614770 \times 10^{-5}$	$\lambda_7 = 0.3886011392 \times 10^{-5}$	$\Lambda_7 = 0.5033614770 \times 10^{-5}$
		$\lambda_8 = 0.1094511318 \times 10^{-16}$	$\Lambda_8 = 0.1417738596 \times 10^{-16}$
		$\lambda_9 = 0.1094511318 \times 10^{-16}$	$\Lambda_9 = 0.1417738596 \times 10^{-16}$

Thus, the stability analysis of the symmetric breather in the K_4 chain is reduced to investigation of the stability of the *zero solution* of the equation

$$z'' + \Lambda^2 cn^2(\tau, \tfrac{1}{\sqrt{2}})z(\tau) = 0 \tag{27}$$

for different values of the parameter Λ which are connected with the eigenvalues λ_j of the matrix **A** from Eq. (19). In the following, we will call Eq. (27) the basic equation.

The standard Floquet analysis of the basic equation (27) reveals that its zero solution is stable for $0 < \Lambda \leqslant 1$, $3 \leqslant \Lambda \leqslant 6$, etc., while for $1 < \lambda < 3$, $6 < \Lambda < 10$, etc. this solution is unstable. The boundary values of the parameter Λ ($\Lambda = 0, 1, 3, 6, 10, \ldots$) for which the character of stability is changed correspond to $\Lambda = \frac{1}{2}n(n+1)$ with $n = 0, 1, 2, 3, 4, \ldots$. These boundary values, separating stable and unstable regions of Λ, correspond to the *periodic* solutions[7] of the Lamé equation (27) [38].

The above mentioned properties of the Lamé equation allow us to analyze the breathers' stability with the aid of the eigenvalues λ_j of the matrix **A** of the linearized system (19), because of the one-to-one correspondence (26) between λ_j and Λ_j entering Eq. (25).

On the other hand, the elements of the matrix **A** depend on the parameter β from Eq. (3) which determines the relative strength of the intersite interaction with respect to the on-site interaction. As a consequence, the eigenvalues $\lambda_j = \lambda_j(\beta)$ of the matrix **A** are functions of the β and we have calculated them using the appropriate numeric procedure[8] for sufficiently dense set of points within the interval $0 < \beta \leqslant 1$.

In Table 2, we present $\lambda_j(\beta)$ and $\Lambda_j(\beta)$ for the K_4 chain with $N = 3, 5, 7, 9$ particles for $\beta = 0.3$. From this table, one can see that several first eigenvalues possess significant values and tend to the certain limits when N increases, while the additional λ_j (appearing because of this increase) are very small.

In Fig. 1, we depict the function $\Lambda_j(\beta)$ on the background of the stability diagram of the basic equation (27) (stable region is white, unstable is gray). Naturally, $\Lambda_j(\beta)$ of the more significant values are only depicted in Fig. 1 [the rest $\Lambda_j(\beta)$ are small but *positive* numbers]. One can see that all $\Lambda_j(\beta)$ fall into the interval $0 < \Lambda_j(\beta) \leqslant 3$ which consists of the first region of stability ($0 < \Lambda \leqslant 1$) and the first region of instability ($1 < \Lambda < 3$).

[7]The same property takes place for the boundaries of stable and unstable regions for the Mathieu equation.

[8]We have applied facilities of MAPLE for this purpose.

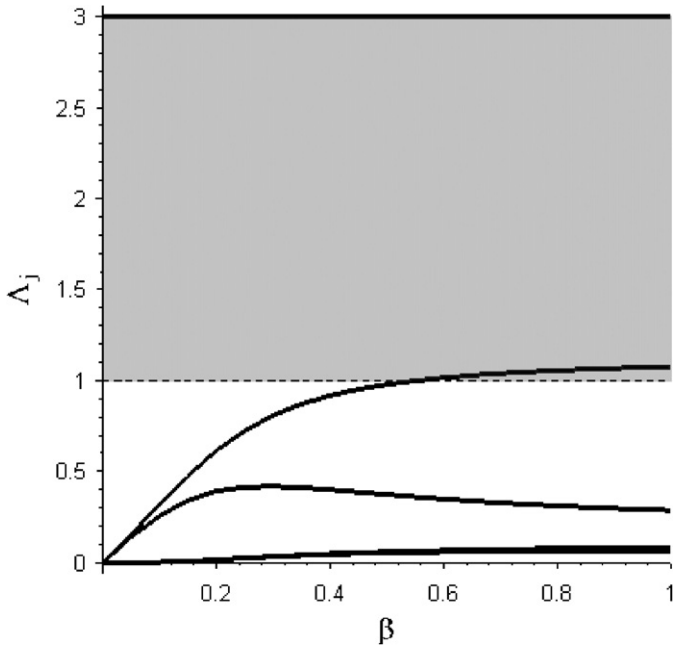

Fig. 1. The parameters Λ_j from the basic equation (27) as functions of the β for the symmetric breathers in the K_4 chain.

Table 3
Spatial profiles $\{\ldots,-\xi_3,-\xi_2,-\xi_1,-\xi_0,\xi_0,\xi_1,\xi_2,\xi_3,\ldots\}$ of the antisymmetric breathers in the K_4 chain with $N=4,6,10$ particles for $\beta=0.3$

	$N=4$	$N=6$	$N=10$
ξ_0	1	1	1
ξ_1	−0.1715728752	−0.1657879024	−0.1657879024
ξ_2		$0.4795767441\times10^{-3}$	$0.4795766628\times10^{-3}$
ξ_3			$-0.1150827549\times10^{-10}$
ξ_4			*

The first eigenvalue $\lambda_1(\beta)$ represents a special case, because corresponding to it $\Lambda_1(\beta)=3$ falls (for any value of β!) *exactly* onto the *boundary* between the first region of instability and the second region of stability. Therefore, a strictly time-periodic solution of the basic equation (27) corresponds to this value of Λ.

It can be verified that the eigenvector $\mathbf{V}_1$ associated with $\lambda_1(\beta)$ is proportional to the spatial profile of our symmetric breather (it describes only small change of the breather amplitude). Obviously, such disturbance *along* the breather solution is not connected with its stability properties and only disturbances in the *transversal* direction are meaningful.

It is clear from Fig. 1 that for $\beta\leqslant\beta_c=0.554\ldots$ all Λ_j fall into the first stability region $0<\Lambda\leqslant1$ and, as a consequence, our symmetric breather is *stable* for such strength of interparticle interaction. On the other hand, one value of the parameter Λ, namely, $\Lambda_2(\beta)$ enters the first unstable region $1<\Lambda<3$ for $\beta>\beta_c$ and the considered breather loses its stability. Thus, the symmetric breather (8) in the K_4 chain turns out to be a stable dynamical object only when the interparticle interaction is not too large with respect to the on-site interaction ($\beta\leqslant\beta_c=0.554\ldots$). Below, we will show that the fully opposite situation takes place for the antisymmetric breather (9).

2.1.2. *Antisymmetric breathers (Page modes)*

Now, let us consider the antisymmetric breather (9) in the K_4 chain. All the above discussed methods for investigating the problems of existence and stability of the symmetric breather (8) are also valid in the present case.

Table 4
The values of the parameter Λ from Eq. (27) for the antisymmetric breathers in the K_4 chain with different number of particles (N)

$N=4$	$N=6$
$\Lambda_1 = 3$	$\Lambda_1 = 3$
$\Lambda_2 = 1.174380299$	$\Lambda_2 = 1.174158240$
$\Lambda_3 = 0.2903225809$	$\Lambda_3 = 0.2706091431$
$\Lambda_4 = 0.2032288097$	$\Lambda_4 = 0.2054306666$
	$\Lambda_5 = 0.2705947721 \times 10^{-2}$
	$\Lambda_6 = 0.2699701623 \times 10^{-2}$
$N=8$	$N=10$
$\Lambda_1 = 3$	$\Lambda_1 = 3$
$\Lambda_2 = 1.174158240$	$\Lambda_2 = 1.174158240$
$\Lambda_3 = 0.2706091431$	$\Lambda_3 = 0.2706091431$
$\Lambda_4 = 0.2054306666$	$\Lambda_4 = 0.2054306666$
$\Lambda_5 = 0.2705931835 \times 10^{-2}$	$\Lambda_5 = 0.2705931835 \times 10^{-2}$
$\Lambda_6 = 0.2699703891 \times 10^{-2}$	$\Lambda_6 = 0.2699703891 \times 10^{-2}$
$\Lambda_7 = 0.2269482819 \times 10^{-8}$	$\Lambda_7 = 0.2269482817 \times 10^{-8}$
$\Lambda_8 = 0.2269482814 \times 10^{-8}$	$\Lambda_8 = 0.2269482782 \times 10^{-8}$
	$\Lambda_9 \sim 10^{-26}$
	$\Lambda_{10} \sim 10^{-26}$

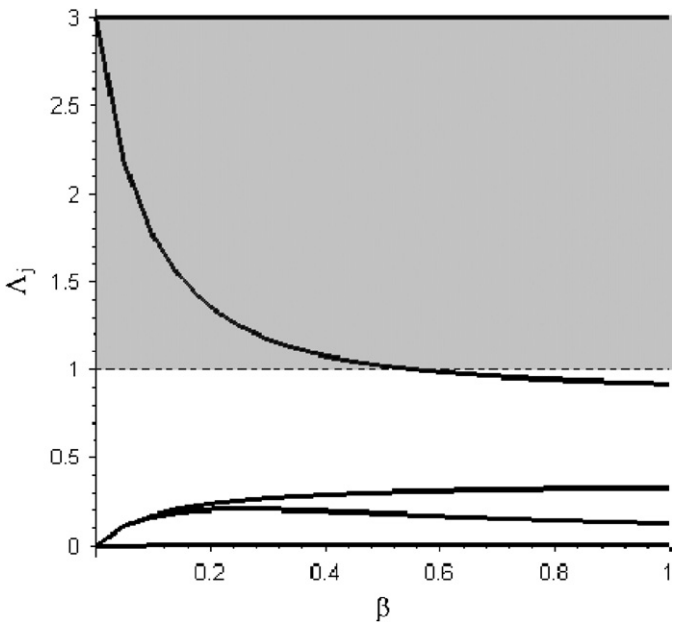

Fig. 2. The parameters Λ_j from the basic equation (27) as functions of the β for the antisymmetric breathers in the K_4 chain.

The spatial profiles for the antisymmetric breather (9) for the K_4 chain with different number of particles (N) and $\beta = 0.3$ are presented in Table 3. The eigenvalues of the matrix $\mathbf{A}$ and the corresponding values of the parameter Λ from the basic equation (27) are listed for some values of N in Table 4.

Finally the significant values of $\Lambda_j(\beta)$ are depicted in Fig. 2 as functions of the parameter β from the dynamical equations (3) of the K_4 model.

Comparing Fig. 1 for the symmetric breather and Fig. 2 for the antisymmetric breather reveals some interesting features of these dynamical objects. Indeed, the antisymmetric breather, unlike the symmetric one,

Table 5
Spatial profiles $\{\xi_4, \xi_3, \xi_2, \xi_1, \xi_0, \xi_0, \xi_1, \xi_2, \xi_3, \xi_4\}$ and the parameters Λ_j from Eq. (27) for the symmetric multibreather in the K_4 chain (3) with $N = 10$ particles for different strength of interparticle interaction (β)

	$\beta = 0.1$	$\beta = 0.2$	$\beta = 0.206$
ξ_0	1	1	1
ξ_1	−0.1272884566	−0.4299888161	−0.5220782231
ξ_2	$0.1811663713 \times 10^{-3}$	0.01080951473	0.0188956596
ξ_3	-0.52×10^{-12}	$-0.1593990593 \times 10^{-6}$	-0.81×10^{-6}
ξ_4	*	*	0.62×10^{-19}
Λ_1	3	3	3
Λ_2	0.3378517129	0.8708501976	0.985358
Λ_3	$0.4210123582 \times 10^{-2}$	0.06780972327	0.094902
Λ_4	0.861×10^{-8}	$0.4420920417 \times 10^{-4}$	0.001277
Λ_5	$\sim 10^{-25}$	0.98×10^{-14}	0.23×10^{-12}

is *unstable* for *small* values of β. This fact can be seen from Fig. 2 because $\Lambda_2(\beta)$ fall into the first region of unstable motion up to the *same critical value* $\beta = \beta_c = 0.554\ldots$. All other values $\Lambda_j(\beta)$ $(j > 2)$ are in the first region of stable motion (the special case $\Lambda_1(\beta) \equiv 3$ we have already discussed in connection with studying the symmetric breather). The most intriguing point is that the critical value β_c for losing the stability of the symmetric breather when β increase from zero and that for acquiring the stability of the antisymmetric breather *coincide* with each other.

Thus the main result can be described as follows. For $\beta < \beta_c = 0.554\ldots$ the symmetric breather (Sievers–Takeno mode) is stable, while the antisymmetric breather (Page mode) is unstable. For $\beta > \beta_c$, the picture is opposite: the symmetric breather is unstable, while the antisymmetric breather is stable.

From the above discussion, we conclude that the symmetric breather is stable when interparticle interaction is weak relative to the on-site interaction, while the antisymmetric breather is stable when this interaction is strong.

2.1.3. Symmetric multibreathers

We have just considered two types of breathers which are frequently discussed in the literature—Sievers–Takeno and Page modes. However, other types of DBs can also exist in the K_4 chain. They represent localized nonlinear normal modes whose spatial profiles are determined by Eqs. (6). As an example, we consider the symmetric multibreather (10) with two particles in its "core" (the coding sequence $\{0, \ldots, 0, 1, 1, 0, \ldots, 0\}$ corresponds to it in the anticontinuous limit). The above discussed methods for DB investigation in the K_4 chain are valid in this case, and we present here only some final results.

The spatial profiles of the considered multibreather for several values of the strength of the interparticle interaction (β) for the K_4 chain with $N = 10$ particles can be seen in Table 5.

The breathers presented in this table possess very strong localization. Their stability is characterized by the parameters Λ_j from the basic equation (27). The value $\Lambda_1 = 3$, as well as for all the above cases, corresponds to an infinitesimal disturbance along the breather and, therefore, does not affect its stability.

On the other hand, Λ_2 tends to the boundary ($\Lambda = 1$) of the first stable region of the basic equation (27) with increasing β, while all the other Λ_j continue to be inside this stable region. Such behavior of $\Lambda_j(\beta)$ can be seen more explicitly from Fig. 3, which is depicted similarly to Figs. 1 and 2.

From this figure, we can conclude that the symmetric multibreather (10) possesses the lesser threshold of stability with respect to the strength of the interparticle interaction (β) in comparison with the simple symmetric breather (8). Indeed, the former loses stability at $\beta = 0.206..$, while the latter loses the stability at $\beta_c = 0.554\ldots$.

2.2. DBs in the chain of the Duffing oscillators with cubic coupling

We consider the dynamical model described by Eqs. (2). These equations differ from those of the K_4 chain by the additional linear term (x_i) in their left-hand side.

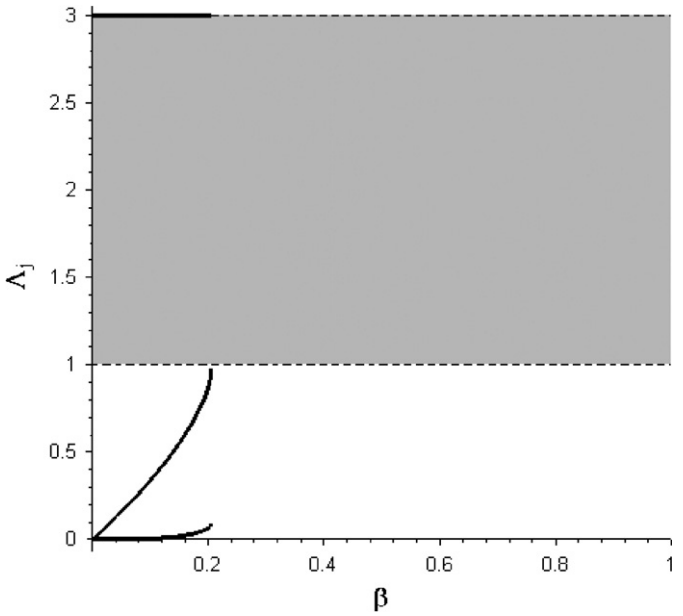

Fig. 3. $\Lambda_j(\beta)$ as functions of the strength of interparticle interaction β for the symmetric multibreather (10) in the K_4 chain (3).

Assuming $x_i(t) = k_i x_1(t)$, one can reveal that nonlinear normal modes exist in this model as well as in the K_4 chain. Moreover, the algebraic equations (6) for determining the spacial profiles $\mathbf{k} = \{k_i \,|\, i = 1, \ldots, N\}$ of NNMs are identical with those for the K_4 chain. Thus, the spatial profiles of DBs in the chain of the Duffing oscillators with cubic coupling (2) fully coincide with those in the K_4 chain (3).

The governing equation which determines the time-evolution of the DBs reads $\ddot{x}_1 + x_1 + p^2(\mathbf{k})x_1^3 = 0$ with $p^2(\mathbf{k})$ being equal to that in the governing equation for the K_4 chain. For the symmetric breather $k_2 = k_N$ and one can obtain [28]:

$$p^2(\mathbf{k}) = 1 + 2\beta(1 - k_2)^3. \tag{28}$$

Actually $p^2(\mathbf{k})$ depends on the number of particles (N) in the chain since all k_i ($i = 1..N$) depend on each other and, therefore, also on N.

Although the breathers for the CD model possess the identical profiles with those of the K_4 chain, their stability properties are different. Let us consider this question in some detail.

As was already emphasized, the stability of the DBs in the K_4 chain does not depend on their amplitudes. Indeed, $\Lambda = \Lambda(\beta)$ from the basic equation (27) is independent of the breather's amplitude A_0 and the stability diagram of its zero solution in the $\Lambda - A_0$ plane looks as depicted in Fig. 4.

Therefore, to any $\Lambda = \Lambda(\beta)$, determined by a certain eigenvalues λ_j of the matrix $\mathbf{A}$ from Eq. (19), corresponds a horizontal line which fully belongs to a stable or unstable strip in Fig. 4.

It is easy to understand that the linearized system in the vicinity of a given DB for the CD model (2) reads

$$\ddot{\boldsymbol{\delta}} = [-I - 3x_1^2(t)\mathbf{A}]\boldsymbol{\delta}, \tag{29}$$

where $\mathbf{A}$ is a matrix *identical* to that for the K_4 chain (see Eq. (19)). Similarly to the latter case, the specific structure of Eq. (29) allows us to find an orthogonal transformation which splits this system of linear differential equations into independent equations

$$\ddot{\tilde{\delta}}_j + [1 + \Lambda_j \cdot x_1^2(t)]\tilde{\delta}_j = 0, \tag{30}$$

where $\Lambda_j = 3\lambda_j/p^2(\mathbf{k})$, while λ_j are eigenvalues of the matrix $\mathbf{A}$.

The stability diagram in $\Lambda - A_0$ plane for zero solution of each Eq. (30) is depicted in Fig. 5. It differs from that of the K_4 chain (see Fig. 4) for small breather amplitudes.

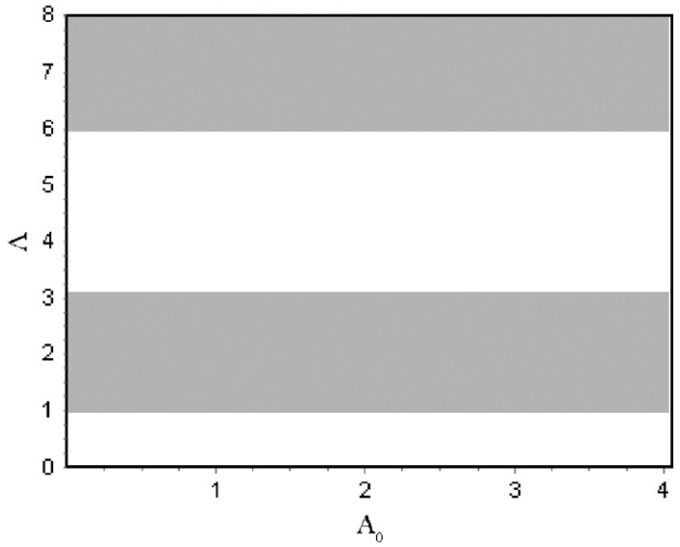

Fig. 4. Stability diagram for the K_4 chain (see Eq. (19)).

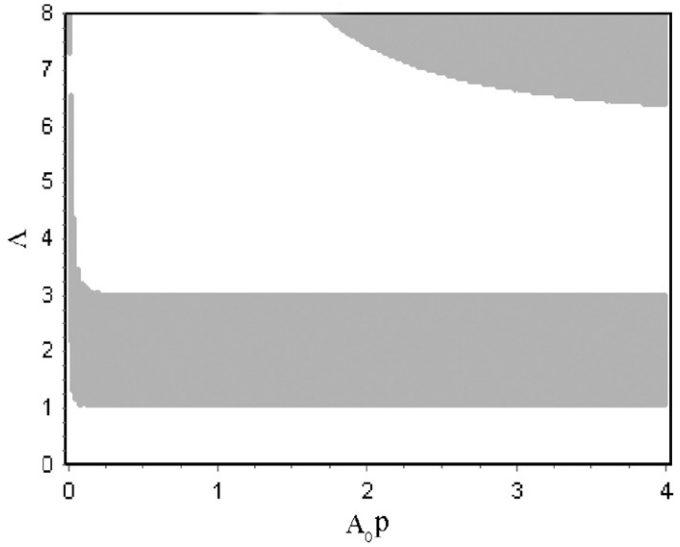

Fig. 5. Stability diagram for the CD model (see Eq. (30)).

A given breather in the CD model will be stable, if all Λ_j for the fixed value of $A_0 \cdot p(\mathbf{k})$ fall into the stable regions shown in Fig. 5 by the gray color.

From the above discussion, we conclude that, unlike the K_4 chain, the stability of the DBs in the CD model do depend on their amplitudes A_0.

3. Pair synchronization method for constructing DBs

Up to this point, we have used the concept of nonlinear normal modes for constructing DBs in the K_4 chain (3) and CD model (2). However, NNMs can only exist in the N-particle mechanical systems with very specific types of interparticle interactions. On the other hand, DBs can exist in vast classes of nonlinear lattices, and some numerical methods were developed for their obtaining with high precision (see Refs. [4,5,27]).

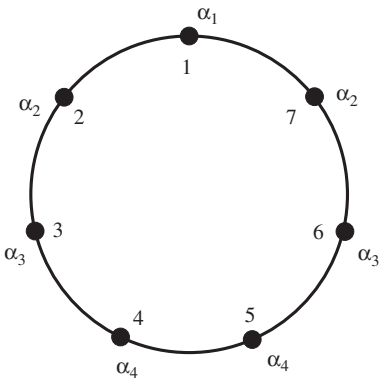

Fig. 6. Numeration of the particles and their initial velocities for the symmetric breather in the chain with $N = 7$.

In Refs. [31,32] we have presented a new method for this purpose which has an explicit physical interpretation. We call it the method of pair synchronization. This method can be used for constructing DBs in different nonlinear Hamiltonian lattices, but we prefer to demonstrate it with the simple case of the chain of linear coupled hard Duffing oscillators (1).

3.1. Algorithm of the pair synchronization method

We will consider the simple symmetric breathers in the chains (1) with $N = 3, 5, 7, 9, \ldots$ particles. Because of the periodic boundary conditions (4), we can imagine that our chain represents a ring (the equilibrium state of the chain with $N = 7$ is depicted in Fig. 6).

We start the exposition of our method with the case of $N = 3$. Let the first particle be the central particle of the breather. Therefore, its amplitude is greater than the amplitudes of the peripheral particles, i.e. $|x_1(t)| > |x_2(t)|$, $|x_3(t)|$. Moreover, the relation $x_2(t) = x_3(t)$ must hold as far as we search for the symmetric breather. To construct such a breather, the following initial conditions can be used for integrating the dynamical equations (1):

$$x_3(0) = x_1(0) = x_2(0) = 0, \quad \dot{x}_1(0) = \alpha_1, \ \ \dot{x}_2(0) = \alpha_2, \ \ \dot{x}_3(0) = \alpha_3.$$

Thus, we suppose that all particles of the chain are in their equilibrium positions at the initial instant, but possess certain velocities which we denote by α_i ($i = 1..N$).

There are two parameters upon which our breathers depend, namely, β, entering the dynamical equations (1), and the initial velocity α_1 of the central breather's particle. Choosing some reasonable values of these parameters and supposing $\alpha_2 = 0$, we integrate equations (1) for $N = 3$ over time interval containing, at least, one zero of the function $x_1(t)$ and one zero of $x_2(t)$ (see Fig. 7a). Now let us *change* the initial velocity $\dot{x}_2(0) = \alpha_2$ of the second particle with the aim of *coincidence* of the first zero of $x_2(t)$ with that of $x_1(t)$. In other words, we try to *synchronize* the oscillations of the first particle $[x_1(t)]$ with those of two neighboring particles $[x_2(t) = x_3(t)]$.

Different numerical methods can be applied for such purpose, for example, the "shooting" method using the idea of dichotomy. Zeros of the functions $x_1(t)$ and $x_2(t)$ can be found by the Newton–Raphson method or by some other well-known numerical methods.

As a consequence of the above synchronization, all the zeros of the functions $x_1(t)$ and $x_2(t)$ coincide with each other and we obtain the symmetric three-particle breather depicted in Fig. 7b. The synchronization of the vibrations of the first and second particles we call the $S[1, 2]$ procedure. A similar procedure for synchronization of the vibrations of the i-th and j-th particles will be called the $S[i, j]$ procedure.

In general case, the algorithm of the discussed method for arbitrary N can be described as follows. We synchronize the vibrations of the particles 1 and 2 with the aid of the above discussed procedure $S[1, 2]$. Then we synchronize the vibrations of the particles 2 and 3 with the aid of the procedure $S[2, 3]$ and so on, up to the

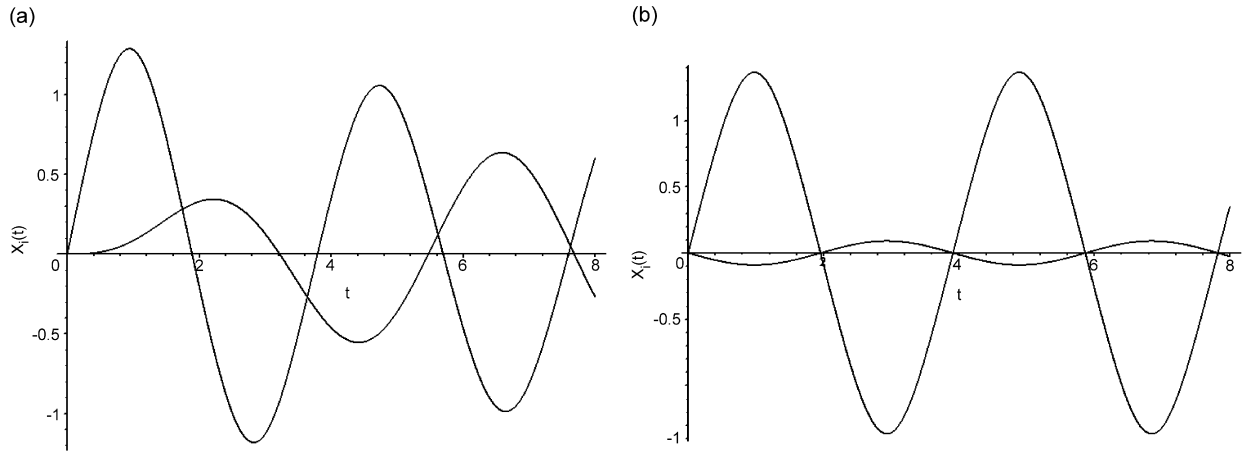

Fig. 7. Pair synchronization method for the chain (1) with $N = 3$: (a) initial stage and (b) final stage.

Table 6
The initial velocities and resulting amplitudes of the breather's particles for the chain (1) with $N = 13$, $\beta = 0.3$

	Initial velocities	Amplitudes
8	0.0003916	0.000197
9	−0.0018250	0.001069
10	0.0076567	0.004485
11	−0.0317182	0.018581
12	0.1312208	0.076913
13	−0.5385204	0.317777
1	2	1.254160
2	−0.5385204	0.317777
3	0.1312208	0.076913
4	−0.0317182	0.018581
5	0.0076567	0.004485
6	−0.0018250	0.001069
7	0.0003916	0.000197

synchronization of the particles $N-1$ and N:

$$\{S[1,2], S[2,3], S[3,4], \ldots, S[N-1,N]\}. \tag{31}$$

The sequence of the pair synchronization procedures (31) must be repeated several times, because synchronization of each next pair of particles can lead to slight disturbance[9] of the preceding pair of particles.

Thus the pair synchronization method represents an iterative process, which we continue up to attaining the desirable level of accuracy. Our numerical calculations show that in many cases the method of pair synchronization rapidly converges even for sufficiently large coupling between oscillators.

3.2. DBs in the chain of the Duffing oscillators with linear coupling

With the aid of the above described pair synchronization method, we have obtained some numerical results for DBs in the chain of coupled Duffing oscillators (1) with different values of the coupling parameter β

[9]At least, for the case of the breather with strong localization.

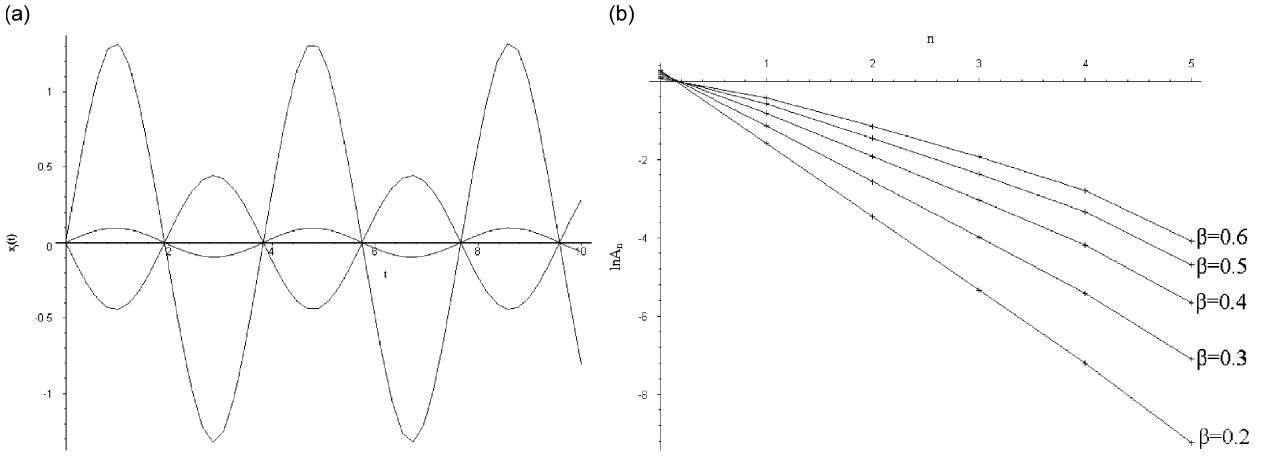

Fig. 8. Discrete breather for the chain (1) with $N = 13$ particles: (a) time evolution $x_i(t)$ of the individual particles and (b) dependence of the breather's localization on the coupling parameter β.

$(0<\beta<10)$. It occurs that in most cases breathers with such values of β are strongly localized and, therefore, to construct them we can consider the chain (1) with sufficiently small numbers of particles N. In Table 6, we present the symmetric DB for model (1) with $N = 13$, $\beta = 0.3$.

The first column of this table contains the numbers of the particles (the first particle is the central particle of the breather). The initial velocities of all the particles are given in the second column (the initial displacements are assumed to be zero), while the amplitudes A_i of vibrations of the particles are given in the third column ($A_i = A_{N-i+2}$ because our breather is symmetric). From Table 6, one can see that the amplitudes of the particles which are the most distant from the breather's center do not exceed 0.02% from the amplitude of the central particle.

The time evolution of the above breather, which is determined by the functions $x_1(t), x_2(t), \ldots, x_N(t)$, is shown in Fig. 8a. Because the amplitudes A_n of the particles decrease rapidly with increasing their distance from the breather center, we depict them in the logarithmic scale for different β in Fig. 8b. From this picture, one can see the *exponential decay* of the amplitudes of the peripheral particles. The degree of the breather spatial localization decreases with increasing β.

The convergence of the pair synchronization method depends essentially on the quality of the initial velocity profile $\alpha = \{\alpha_1, \alpha_2, \alpha_3, \ldots, \alpha_N\}$ from which we begin the calculations along with the algorithm of the method. Some estimations for the initial profile α_{init} for the case of weak interparticle interactions (small value of β) have been proposed in Ref. [31].

Naturally, starting from the small β, we can increase step by step the strength of the interparticle interactions using the final velocity profile for a given β as the initial profile for the next value of β. We can also use the velocity profile which was found for the chain with relatively small number (N) of the particles in the chain as the initial profile for the chain with $N + 2$ particles, etc. Finally, it is possible to change the sequence of the pair synchronization procedures $S[i,j]$ in the iterative cycle (31) for improving the convergence of the considered method.

In any case, we can find DBs in the LD model (1) with sufficiently large values β (even for $\beta \gtrsim 30$). However, the velocity profiles $\alpha(\beta)$ [as well as the spatial profiles] of the symmetric breathers tend with a good accuracy to a certain limit vector α_{lim}, when β becomes larger than 15. Due to this reason, in Table 7, we present the velocity breather profiles only up to $\beta = 10$.

Some similar results for antisymmetric breathers in the LD model (1) are presented in Table 8. For large β the delocalization of the breather vibrations takes place and the spatial profiles of antisymmetric breathers tend to the π-mode $\{-1, 1, -1, 1, -1, 1, \ldots\}$.

For studying the stability of the breathers in the LD chain, we can use the standard Floquet method. As an example, in Fig. 9 we depict the Floquet multiplicators on the unit circle for two examples. From these picture,

Table 7
Velocity profiles for symmetric breathers in the LD model (1) for different values of interparticle interaction (β)

	$\beta = 0.5$	$\beta = 1$	$\beta = 3$	$\beta = 6$	$\beta = 10$
α_5	−0.1032882638	−0.2893006151	−0.4214517416	−0.4387945325	−0.4427417430
α_6	0.3994420656	0.9193077069	1.203400713	1.235644985	1.242822155
α_7	−1.010628378	−1.609666653	−1.781897026	−1.796848651	−1.800079430
α_1	2	2	2	2	2
α_2	−1.010628378	−1.609666653	−1.781897026	−1.796848651	−1.800079430
α_3	0.3994420656	0.9193077069	1.203400713	1.235644985	1.242822155
α_4	−0.1032882638	−0.2893006151	−0.4214517416	−0.4387945325	−0.4427417430

Table 8
Velocity profiles for antisymmetric breathers in the LD model (1) for different values of interparticle interaction (β)

	$\beta = 0.1$	$\beta = 0.3$	$\beta = 0.5$	$\beta = 0.7$	$\beta = 0.9$	$\beta = 0.97$
α_5	0.01125942	0.122897	0.395655	0.8492010	1.439248	1.665248
α_6	−0.1496424	−0.471428	−0.841867	−1.2648100	−1.686680	−1.821661
α_1	2	2	2	2	2	2
α_2	−2	−2	−2	−2	−2	−2
α_3	0.1496424	0.471428	0.841867	1.2648100	1.686680	1.821661
α_4	−0.01125942	−0.122897	−0.395655	−0.8492010	−1.439248	−1.665248

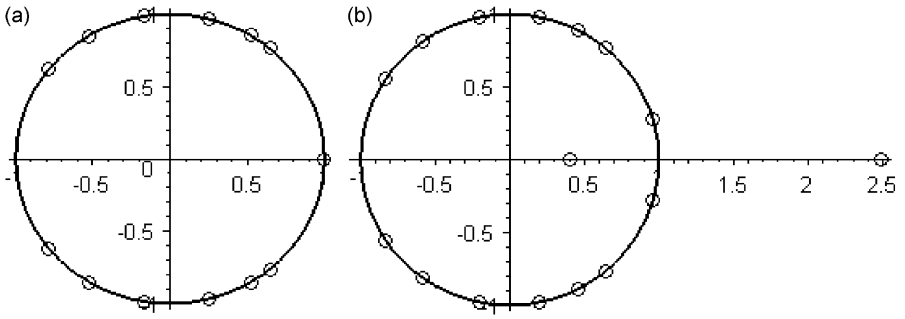

Fig. 9. The Floquet multiplicators for DBs in LD model (1) with $\beta = 0.3$: (a) symmetric breather $\{N = 7,\ \alpha_1 = 2,\ \alpha_2 = -0.538056,\ \alpha_3 = 0.129355,\ \alpha_4 = -0.024052\}$ and (b) antisymmetric breather $\{N = 8,\ \alpha_1 = 2,\ \alpha_2 = -0.466790,\ \alpha_3 = 0.101999,\ \alpha_4 = -0.026418\}$.

one can see that the symmetric breather with $N = 7$, $\alpha_1 = 2$, $\alpha_2 = -0.538056$, $\alpha_3 = 0.129355$, $\alpha_4 = -0.024052$, $\beta = 0.3$ is stable, while the antisymmetric breather with $N = 8$, $\alpha_1 = 2$, $\alpha_2 = -0.466790$, $\alpha_3 = 0.101999$, $\alpha_4 = -0.026418$, $\beta = 0.3$ is unstable.

3.3. Quasibreathers

Because of the spatial localization of a given breather, the different particles of the chain vibrate with essentially different amplitudes. On the other hand, it is typical for nonlinear dynamics, that different frequencies correspond to the particles vibrating with different amplitudes. Therefore, the natural question arises: ''How can such properties as spatial localization and strict time-periodicity coexist in breather vibrations''?

Using the pair synchronization method, we synchronize the vibrations of central particles with those of the peripheral particles. In Ref. [31], we have demonstrated (with some additional approximation) that this method leads to a very simple physical interpretation of the possibility of the exact breathers'

existence. It turns out that constructing a strictly time-periodic breather, we actually demand annihilation of the contributions with natural vibrational frequencies from all the peripheral particles to the breather solution. This means the existence of some kind of dictatorship of the central particle (in general, of the breather core) which "suppresses any individuality" of the peripheral particles by above-mentioned annihilation. In other words, all terms of the exact breather solution with frequencies different from the frequency of the central particle (which appear from the natural frequencies of the peripheral particles) must necessarily go to zero. The breather core compels the peripheral particles to vibrate with its own frequency. We also demonstrated, for the case of weakly coupled oscillatory chains, that this compulsion leads to the exponential decay of the vibrational amplitudes of the peripheral breather's particles.

For every oscillatory chain considered in the present paper there exists a certain 1D family of DBs which can be parameterized by the breather amplitude (the amplitude of the central particle or particles). To obtain an exact breather, we must strictly tune the initial conditions onto the corresponding 1D manifold in the multidimensional phase space—the space of all possible initial coordinates and velocities of all the particles of the mechanical system. Obviously, this is impossible in any physical experiment. Therefore, we always deal with a certain *vicinity* of the DB but not with the exact breather itself.

On the other hand, if we do not tune the initial conditions onto the *exact* breather solution, i.e. if the vibrational contributions from the peripheral particles are not equal to zero, we will obtain a certain *quasibreather* [28]. This spatially localized dynamical object is characterized by different frequencies appearing from the peripheral particles. The difference in frequencies is brought about by the phenomenon typical for nonlinear dynamics, namely, by the dependence of the frequency on the vibrational amplitude.

In Ref. [28], we proposed to characterize the proximity of the quasibreather to an exact time-periodic breather with the aid of the mean square deviations in frequencies of the individual particles and that of the fixed particle in time (there exist a certain temporal drift of the frequency of every chosen particle). We also presented there some arguments (at least, for the case of the K_4 chain) for the possibility of the quasibreather stability despite of the absence of the time periodicity. However, we cannot present any refined mathematical proof on quasibreather stability for infinite time.

On the other hand, one often reveals that the lifetime of a quasibreather, if it actually decays in time, can be exponentially large for small deviations from the exact breather. For example, in Fig. 10, we depict the time evolution of the quasibreather in the weakly coupled Duffing chain which lives, at least, up to $t \sim 10^6$.

Finally, since we cannot tune exactly on the strictly time periodic breather solution in any physical experiment (and even in numerical experiments), quasibreathers seem to be much more relevant spatially localized dynamical objects than the exact DBs. Some additional details for this point of view can be found in Ref. [28].

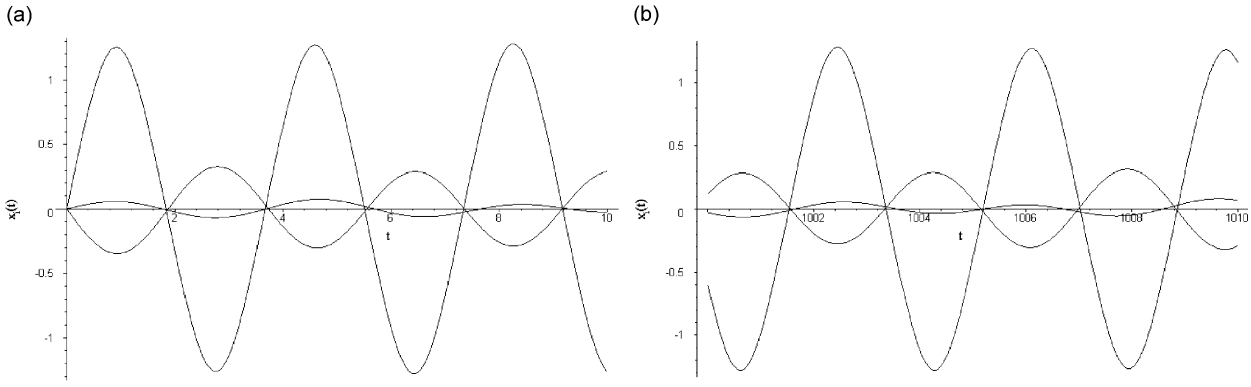

Fig. 10. An extremely long-lived quasibreather for the Duffing chain (1) with $N = 5$ particles which, possibly, is a stable dynamical object [$\gamma = 0.3$, $\alpha_1 = 2$, $\alpha_2 = -0.5760$, $\alpha_3 = 0.1$].

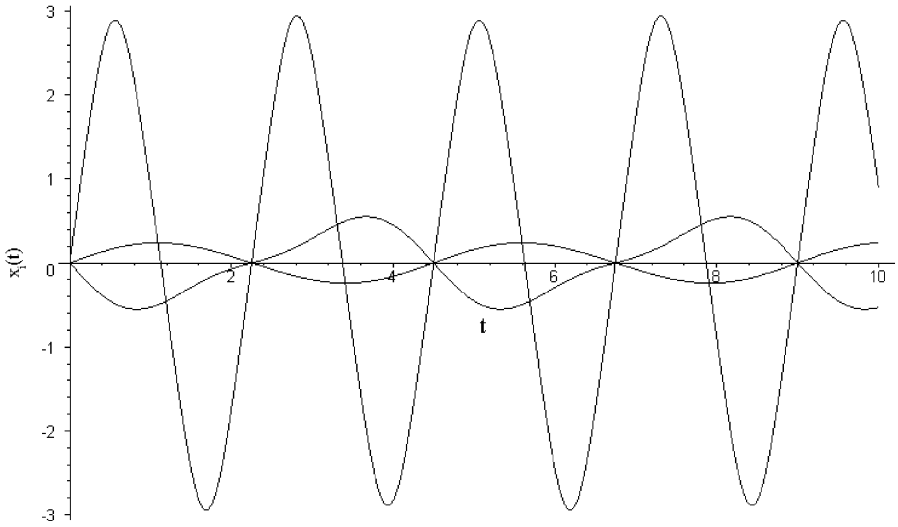

Fig. 11. Two-frequency symmetric breather in the Duffing chain (1) for $\beta = 0.3$, $\alpha_1 = 7$, $N = 5$.

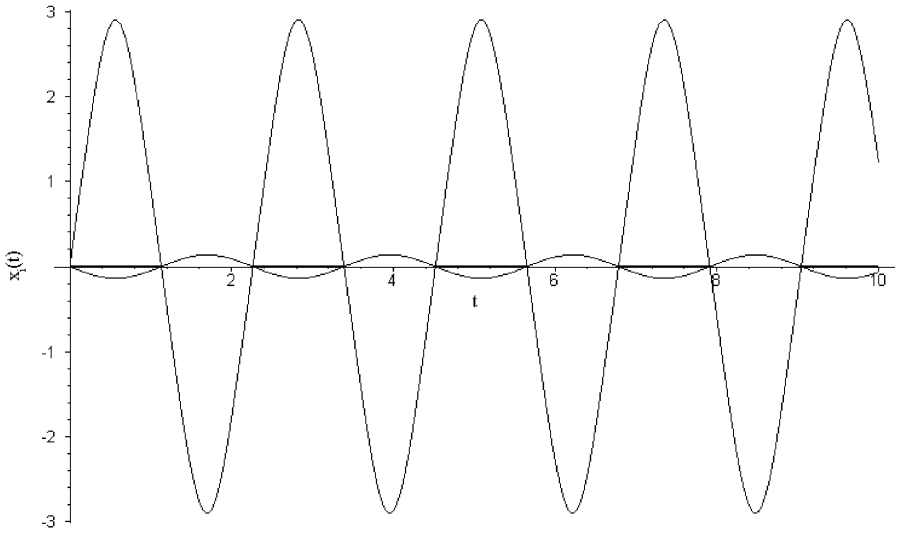

Fig. 12. Single-frequency symmetric breather in the Duffing chain (1) for $\beta = 0.3$, $\alpha_1 = 7$, $N = 5$. Vibrations of the third particle is not visible, because of its small amplitude.

4. Many-frequency DBs

Now we consider the many-frequency breathers which were mentioned in the Introduction. Let us remember that we use this term for such spatially localized dynamical objects whose particles vibrate with several *different* but *commensurate* frequencies. This means that many-frequency breather proves to be a *time-periodic* object whose period T is the largest of the multiple periods $T_1, T_2, \ldots, T_N$ of all the particles of the chain.

4.1. The chain of Duffing oscillators with linear coupling

Several many-frequency DBs for this model have already been found in Ref. [31]. Below we consider some of them as well as a number of additional examples, in particular, the many-frequency symmetric breather.

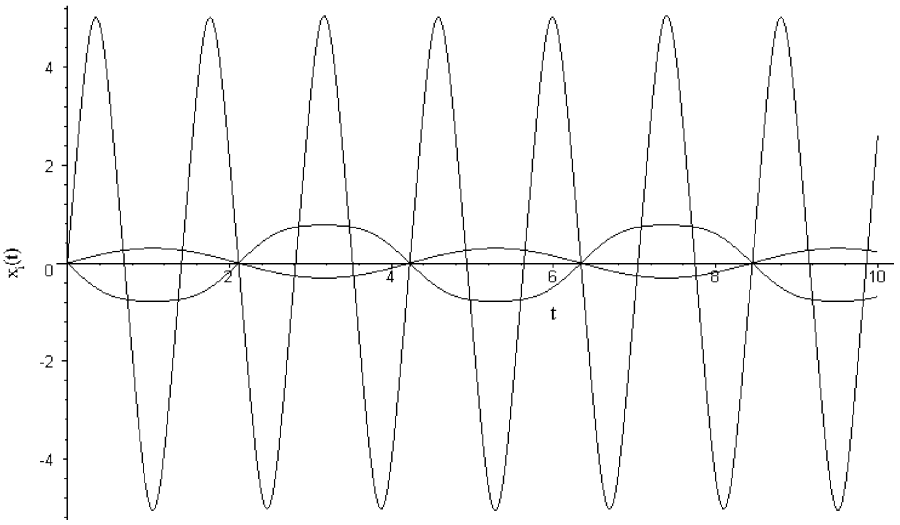

Fig. 13. Two-frequency symmetric breather in the Duffing chain (1) for $\beta = 0.3$, $\alpha_1 = 19$, $N = 5$ ($\omega_1 = 3\omega_2 = 3\omega_3$). This breather is unstable.

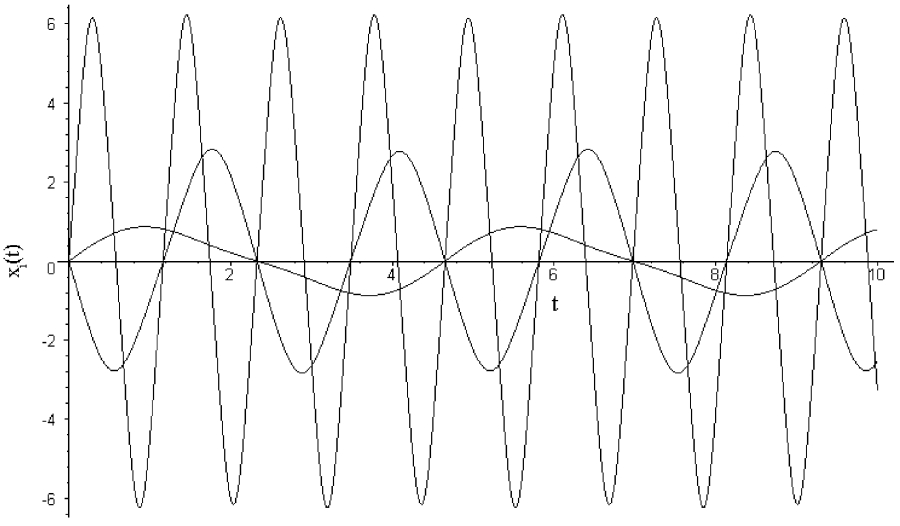

Fig. 14. Three-frequency symmetric breather in the Duffing chain (1) for $\beta = 0.3$, $\alpha_1 = 28$, $N = 5$ ($\omega_1 = 2\omega_2 = 4\omega_3$). This breather is unstable.

In Fig. 11, we depict a *two-frequency* symmetric breather ($\omega_1 = 2\omega_2 = 2\omega_3$) in the chain (1) with $N = 5$ particles for $\beta = 0.3$. Indeed, the first particle $[x_1(t)]$ vibrates with the frequency twice larger than those of all the other particles $[x_2(t),\ x_3(t)]$. This breather with $\omega_b = \omega_2 (= \omega_3) = 1.39615$ corresponds to the following data: $\beta = 0.3$, $\alpha_1 = 7$, $\alpha_2 = -1.064224$, $\alpha_3 = 0.352247$. Hereafter, we do not point out explicitly that all the initial displacements are zero: $x_i(0) = 0$, $i = 1..N$.

Note that for the same β and α_1, we can also find a *single-frequency* symmetric breather with $\omega_1 = \omega_2 = \omega_3 = 2.77828$ (see Fig. 12 which was obtained for $\beta = 0.3$, $\alpha_1 = 7$, $\alpha_2 = -0.379206$, $\alpha_3 = 0.017876$, $N = 5$).

In Fig. 13, we depict the *two-frequency* symmetric breather with $\omega_b = \omega_2 = 1.48666$ whose particles vibrate with the following frequencies: $\omega_1 = 3\omega_2 = 3\omega_3$. This breather corresponds to the following initial data: $\alpha_1 = 19$, $\alpha_2 = -1.593445$, $\alpha_3 = 0.456080$ ($N = 5$, $\beta = 0.3$).

In Fig. 14, the *three-frequency* symmetric breather with $\omega_1 = 2\omega_2$, $\omega_2 = 2\omega_3$ is shown. It corresponds to the following initial data: $\alpha_1 = 28$, $\alpha_2 = -7.018426$, $\alpha_3 = 1.472607$ ($N = 5$, $\beta = 0.3$). The breather frequency is $\omega_b = \omega_3 = 1.35108$.

In Fig. 15, we depict the antisymmetric breather in the chain (1) with $N = 6$ particles for $\beta = 0.3$. The relation between the vibration frequencies of the individual particles reads $\omega_1 = 2\omega_2 = 2\omega_3$, while the breather frequency is $\omega_b = \omega_2 = 1.653176$. The initial velocity profile for this breather is $\alpha_1 = 10$, $\alpha_2 = -2.199936$, $\alpha_3 = 0.947441$ ($N = 5$, $\beta = 0.3$).

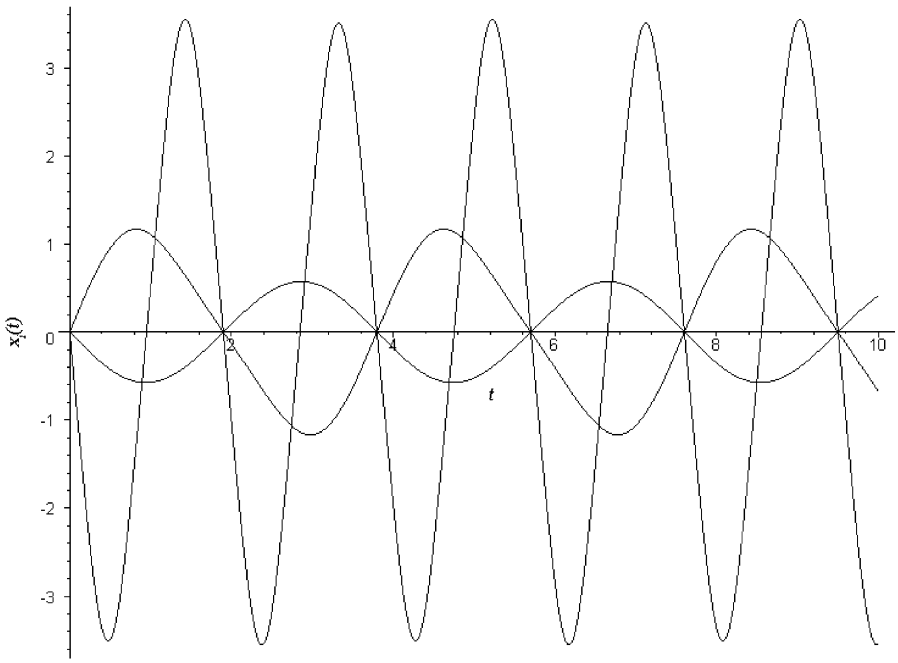

Fig. 15. Two-frequency antisymmetric breather in the Duffing chain (1) for $\beta = 0.3$, $\alpha_1 = 10$, $N = 5$ ($\omega_1 = 2\omega_2 = 2\omega_3$).

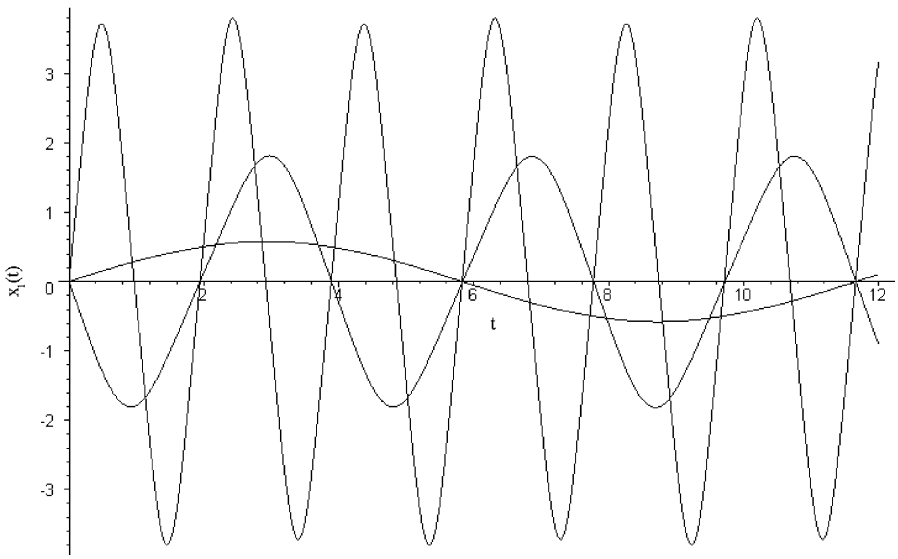

Fig. 16. Three-frequency symmetric breather in the K_4 chain (3) for $\beta = 0.01$, $\alpha_1 = 10$, $N = 5$.

Note that the pair synchronization method providing us with an initial breather profile does not guarantee the breather stability. For example, the breathers depicted in Figs. 13 and 14 prove to be unstable dynamical objects, and this fact can be checked by straightforward integration of the dynamical equation (1), as well as with the aid of the Floquet method.

Note that, for simplicity, in many examples of this section we consider only chains with small numbers of particles (N). This is not an essential restriction because, in every such case, the synchronization procedure can be easily continued for much greater values of N.

Let us emphasize that, unlike the terminology of the paper [26], our *many-frequency* breathers *are time-periodic* dynamical objects, but different particles vibrate with different (divisible) frequencies ω_i ($i = 1..N$). We would like to note that one can find in Ref. [1] a certain mention of multibreathers whose particles vibrate with different but commensurate frequencies. However, we do not know any papers with detailed analysis of such dynamical objects and it seems that our many-frequency breathers are not fully identical to the above mentioned multibreathers.

4.2. The K_4 chain

Using the pair synchronization method, we can construct many-frequency breathers for different nonlinear Hamiltonian lattices, in particular, for the chains (2) and (3). These chains represent a certain interest for our discussion because they admit the existence of nonlinear normal modes which correspond only to single-frequency breathers. Let us consider this question in more details.

In Fig. 16 we depict the many-frequency breather for the K_4 chain with $N = 5$ and $\beta = 0.01$. The initial velocity profile for this DB is [$\alpha_1 = 10$, $\alpha_2 = -2.738135$, $\alpha_3 = 0.308056$]. It can be seen from Fig. 16 that $\omega_1 = 2\omega_2 = 6\omega_3$ ($\omega_3 = 0.53882$).

Unlike the single-frequency breathers representing nonlinear normal modes, the many-frequency breathers in the K_4 chain are *not* the modes of this type. Indeed, one can see from Fig. 16 that for certain instant t, $x_1(t) = 0$, while $x_2(t)$ and $x_3(t)$ are not zero. Therefore, the main property of the nonlinear normal modes, i.e. $x_i(t) = k_i x_1(t)$, $k_i = const$, is not valid for the many-frequency breathers. This idea is also illustrated by Fig. 17 where we depict the time-evolution of the ratio $x_2(t)/x_1(t)$.

With the aid of the pair synchronization method, we can also construct the many-frequency breathers for the chain of the Duffing oscillators with cubic coupling (2).

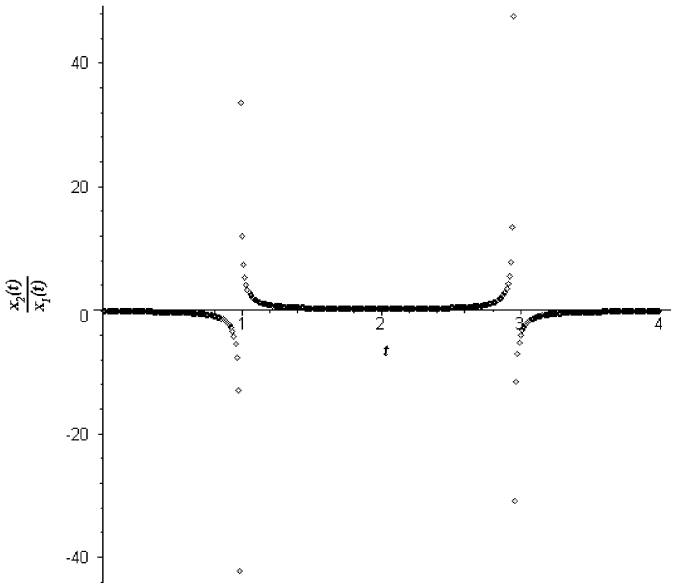

Fig. 17. The time evolution of the ratio $x_2(t)/x_1(t)$ for the three-frequency symmetric breather in the K_4 chain depicted in Fig. 16.

5. Conclusions

For the chain with uniform on-site and intersite potential of the fourth order (K_4 chain (3)), we have constructed some DBs, in terms of nonlinear normal modes and analyzed their stability with respect to the strength of the interparticle interaction (coefficient β from Eq. (3)). It turns out that symmetric breather (Sievers–Takeno mode) and antisymmetric breather (Page mode) change their stability properties at the same critical point $\beta_c = 0.554\ldots$. Namely, the symmetric breather, being stable for $\beta<\beta_c$, becomes unstable for $\beta>\beta_c$, while the antisymmetric breather being unstable for $\beta<\beta_c$, becomes stable for $\beta>\beta_c$. On the other hand, the simple symmetric multibreather (10) is more sensitive to increasing the interparticle interaction: already it loses the stability for $\beta \approx 0.206$.

In the K_4 chain, the stability of the DBs is independent of their amplitudes and depends only on β. The breathers in the chain of the Duffing oscillators with cubic coupling (2) also represent localized nonlinear normal modes, but their stability, unlike the case of the K_4 chain, depends on their amplitudes and the strength of the interparticle interaction (β).

Note that a part of the above mentioned results was presented in our previous papers [28,31]. In contrast to the discussed models (2) and (3), localized nonlinear normal modes do not exist in the chain of the linear coupled Duffing oscillators (1) and we have to search for DBs for this case in different manner.

In Refs. [31,32] the pair synchronization method have been proposed for constructing DBs in arbitrary nonlinear Hamiltonian lattices. In the present paper, we use this method to obtain DBs of different types when their construction is impossible in terms of nonlinear normal modes.

In this way, we have constructed single-frequency DBs, as well as a number of many-frequency breathers in the chain of the linear coupled Duffing oscillators. Unlike the conventional (single-frequency) breather, in many-frequency DBs, different chain particles vibrate with *different but commensurate* frequencies. We have already noted in the introduction that we are not aware of any detail investigation of these dynamical objects, although some references to the possibility of their existence can be found in the literature in connection with discussions of the multibreathers (see, for example, Ref. [1]).

We have demonstrated that many-frequency breathers *are not* nonlinear normal modes even in the cases where localized nonlinear normal modes of such type do exist (they represent only single-frequency DBs).

Finally, we have discussed some aspects of quasibreathers which were introduced in Ref. [28] as generalization of the concept of DBs. Such spatially localized dynamical objects are not strictly time-periodic entities: different particles of the chain vibrate with slightly different frequencies and these frequencies slightly drift in time. Quasibreathers seem to be more adequate dynamical objects than the strictly time-periodic DBs since it is impossible to tune exactly onto the latter in any physical experiments.

Acknowledgments

We are very grateful to Prof. V.P. Sakhnenko for his friendly support and to Prof. Yu.V. Mikhlin for hospitality during our visit to Kharkov in September 2007. The authors gratefully thank N.A. Zemlyanova for her valuable linguistic consultations. This work has been supported by a grant from Southern Federal University (Russia, 2008). G.S.D. is very grateful to the Russian foundation "Dynasty" for some financial support.

References

[1] S. Aubry, Breathers in nonlinear lattices: existence, linear stability and quantization, *Physica D* 103 (1997) 201–250.
[2] S. Flach, C.R. Willis, Discrete breathers, *Physics Reports* 295 (1998) 181–264.
[3] S. Aubry, Discrete breathers: localization and transfer of energy in discrete Hamiltonian nonlinear systems, *Physica D* 216 (2006) 1–30.
[4] S. Flach, Computational studies of discrete breathers, in: T. Dauxois, A. Litvak-Hinenzon, R. MacKay, A. Spanoudaki (Eds.), *Energy Localization and Transfer*, World Scientific, Singapore, 2004, pp. 1–71.
[5] S. Flach, A. Gorbach, Discrete breathers: advances in theory and applications, *Physics Reports* (2007), submitted.
[6] M. Sato, A.J. Sievers, Direct observation of the discrete character of intrinsic localized modes in an antiferromagnet, *Nature* 432 (2004) 486–488.

[7] A. Trombettoni, A. Smerzi, Discrete solitons and breathers with dilute Bose–Einstein condensates, *Physical Review Letters* 86 (2001) 2353–2356.
[8] E.A. Ostrovskaya, Yu.S. Kivshar, Matter-wave gap solitons in atomic band-gap structures, *Physical Review Letters* 90 (2003) 160407-4.
[9] E. Trias, J.J. Mazo, T.P. Orlando, Discrete breathers in nonlinear lattices: experimental detection in a Josephson array, *Physical Review Letters* 84 (2000) 741–744.
[10] P. Binder, D. Abraimov, A.V. Ustinov, S. Flach, Y. Zolotaryuk, Observation of breathers in Josephson ladders, *Physical Review Letters* 84 (2000) 745–748.
[11] M. Sato, B.E. Hubbard, A.J. Sievers, B. Ilic, D.A. Czaplewski, H.G. Craighead, Observation of locked intrinsic localized vibrational modes in a micromechanical oscillator array, *Physical Review Letters* 90 (2003) 044102-4.
[12] M. Sato, B.E. Hubbard, A.T. Sievers, Nonlinear energy localization and its manipulation in micromechanical oscillator arrays, *Reviews of Modern Physics* 78 (2006) 137–157.
[13] R. Stearrett, L.Q. English, Experimental generation of intrinsic localized modes in a discrete electrical transmission line, *Journal of Physics D: Applied Physics* 40 (2007) 5394–5398.
[14] M. Peyrard, A.R. Bishop, Statistical mechanics of a nonlinear model for DNA denaturation, *Physical Review Letters* 62 (1989) 2755–2758;
M. Peyrard, Nonlinear dynamics and statistical physics of DNA, *Nonlinearity* 17 (2004) R1–R40.
[15] L.I. Yakushevich, A.V. Savin, L.I. Manevitch, Nonlinear dynamics of topological solitons in DNA, *Physical Review E* 66 (2002) 016614-29.
[16] G.P. Tsironis, If discrete breathers is the answer, what is the question?, *Chaos* 13 (2003) 657–666.
[17] M. Cadoni, R. De Leo, G. Gaeta, A composite model for DNA torsion dynamics, *Physical Review E* 75 (2007) 021919-21.
[18] Yu.A. Kosevich, New soliton equation and exotic localized modes in anharmonic lattices, *Physics Letters A* 173 (1993) 257–262;
Yu.A. Kosevich, Nonlinear sinusoidal waves and their superposition in anharmonic lattices, *Physical Review Letters* 71 (1993) 2058–2061.
[19] T. Cretegny, T. Dauxois, S. Ruffo, A. Torcini, Localization and equipartition of energy in the β-FPU chain: chaotic breathers, *Physica D* 121 (1998) 109–126.
[20] S. Flach, K. Kladko, Moving discrete breathers?, *Physica D* 127 (1999) 61–72.
[21] V.V. Mirnov, A.J. Lichtenberg, H. Guclu, Chaotic breather formation, coalescence and evolution to energy equipartition, *Physica D* 157 (2001) 251–282.
[22] Yu.A. Kosevich, R. Khomeriki, S. Ruffo, Supersonic discrete kink-solitons and sinusoidal patterns with ''magic'' wavenumber in anharmonic lattices, *Europhysics Letters* 66 (2004) 21–27.
[23] B.F. Feng, Y.S. Chan, Intrinsic localized modes in a three particle Fermi–Pasta–Ulam lattice with on-site harmonic potential, *Mathematics and Computers in Simulation* 74 (2007) 292–301.
[24] Yu.A. Kosevich, L.I. Manevitch, A.V. Savin. Wandering breathers and self-trapping in weakly coupled nonlinear chains: classical counterpart of macroscopic tunneling quantum dynamics, arXiv:0705.1957v2 (nlin.PS).
[25] A.A. Ovchinnikov, Localized long-lived vibrational states in molecular crystals, *Soviet Physics JETP* 30 (1970) 147–150.
[26] S. Flach, Conditions on the existence of localized excitations in nonlinear discrete systems, *Physical Review E* 50 (1994) 3134–3142.
[27] J.L. Marin, S. Aubry, Breathers in nonlinear lattices: numerical calculation, from the anticontinuous limit, *Nonlinearity* 9 (1998) 1501–1528.
[28] G.M. Chechin, G.S. Dzhelauhova, E.A. Mehonoshina, Quasibreathers as a generalization of the concept of discrete breathers, *Physical Review E* 74 (2006) 036608-15.
[29] D. Bambusi, D. Vella, Quasi periodic breathers in Hamiltonian lattices with symmetries, *Discrete and Continuous Dynamical Systems—Series B* 2 (2002) 389–399.
[30] R.M. Rosenberg, The normal modes of nonlinear *n*-degree-of-freedom systems, *Journal of Applied Mechanics* 29 (1962) 7–14.
[31] G.M. Chechin, G.S. Dzhelauhova, Construction of the discrete breathers and a simple physical interpretation of their existence, 2007, arXiv:0711.4842v1 (nlin.PS).
[32] P.P. Goncharov, G.S. Dzhelauhova, G.M. Chechin, Breathers in nonlinear monoatomic chains (in Russian), *Izvestiya VUZ: Applied Nonlinear Dynamics* 6 (2007).
[33] Yu.S. Kivshar, Intrinsic localized modes as solitons with a compact support, *Physical Review E* 48 (1993) R43–R45.
[34] S. Flach, Existence of localized excitations in nonlinear discrete systems, *Physical Review E* 51 (1995) 1503–1507.
[35] B. Dey, M. Eleftheriou, S. Flach, G.P. Tsironis, Shape profile of compact-like discrete breathers in nonlinear dispersive lattice systems, *Physical Review E* 65 (2001) 017601-4.
[36] A.V. Gorbach, S. Flach, Compact-like discrete breathers in systems with nonlinear and nonlocal dispersive terms, *Physical Review E* 72 (2005) 056607-9.
[37] M. Abramowitz, I.A. Stegun (Eds.), *Handbook of Mathematical Functions*, Dover Publications Inc., New York, 1965.
[38] E.T. Whittaker, G.N. Watson, *A Course of Modern Analysis*, fourth ed., Cambridge University Press, Cambridge, 1952.